A patchwork pathway of apparently recent origin enables degradation of the synthetic buffer compound TRIS in bacteria.

Johannes Holert[1*], Aron Borker[1], Laura Nübel[1], Rolf Daniel[2], Anja Poehlein[2], Bodo Philipp[1,3]

[1] Institute for Molecular Microbiology and Biotechnology, Microbial Biotechnology & Ecology group, University of Münster, Münster, Germany

[2] Institute for Microbiology and Genetics, University of Göttingen, Göttingen, Germany

[3] Environmental Microbiology, Fraunhofer Institute for Molecular Biology and Applied Ecology, Schmallenberg, Germany

* Corresponding authors: Johannes Holert, Bodo Philipp

Email: johannes.holert@uni-muenster.de

Author Contributions: JH conceived the study, designed, planned, and performed experiments, supervised the work, analysed data, and wrote the manuscript. AB performed cloning, conjugation, and isolation experiments and analysed data. LN performed isolation and growth experiment and analysed data. RD contributed reagents and analytic tools. AP performed DNA and RNA extractions, library preparation, DNA sequencing, and transcriptome analysis, and edited the manuscript. BP conceived the study, supervised the work, co-wrote the manuscript, and supplied funding. All authors have approved the final version.

Competing Interest Statement: The authors declare no conflict of interest.

Keywords: TRIS, bacterial catabolism, pathway evolution, horizontal gene transfer, Pseudomonas

Abstract

The widely used synthetic buffer compound TRIS was long considered to be biologically inert. Herein, we describe the discovery of a complete bacterial degradation pathway for TRIS. By serendipity, a *Pseudomonas* strain was isolated from sewage sludge that was able to grow with TRIS as only carbon and nitrogen source. Genome and transcriptome analyses revealed two adjacent gene clusters embedded in a mobile genetic element on a conjugative plasmid to be involved in TRIS degradation. Conjugational transfer of this plasmid into *P. putida* KT2440 enabled this strain to grow with TRIS, demonstrating that the complete TRIS degradation pathway can be transmitted by horizontal gene transfer. Heterologous gene expression revealed cluster I to encode a TRIS uptake protein, a TRIS alcohol dehydrogenase, and a TRIS aldehyde dehydrogenase, catalyzing the oxidation of TRIS into 2-hydroxymethylserine. Gene cluster II encodes a methylserine hydroxymethyltransferase and a D-serine dehydratase which plausibly catalyze the conversion of 2-hydroxymethylserine into pyruvate. Subsequent enrichments from wastewater purification systems led to the isolation of further TRIS-degrading bacteria from the *Pseudomonas* and *Shinella* genera carrying highly similar TRIS degradation gene clusters.

Our data indicate that TRIS degradation evolved recently via gene recruitment and enzyme adaptation from multiple independent metabolic pathways and database searches suggest that the TRIS degradation pathway is now globally distributed. Our study illustrates how engineered environments can enhance the emergence of new microbial metabolic pathways in short evolutionary time scales. This knowledge is valuable for developing new water purification processes in times of increasing water scarcity.

Introduction

Since the beginning of the industrial revolution hundreds of thousands of new pesticides, herbicides, medical drugs, and other industrial chemicals were synthesized to meet the growing demand of newly emerging agricultural, pharmaceutical, and industrial applications [1]. Many of these anthropogenic chemicals eventually end up in the environment, where their removal is initially restricted due to the absence of efficient biological degradation mechanisms. However, more and more degradation pathways for chemicals that were introduced in the early twentieth century are now being discovered in microbes, suggesting that functional mineralization pathways can evolve within decades after the initial exposure of the microbial community [2]. A prominent example is the degradation pathway for the anthropogenic herbicide atrazine, which has evolved in the genus *Pseudomonas* around fifty years after the large scale introduction of atrazine to the market, enabling these bacteria to exploit this compound as a carbon and nitrogen source for growth [3]. Similarly, catabolic mineralization pathways for other industrially relevant compounds that were introduced in the early twentieth century including herbicides, pesticides, food additives, and medical drugs are now found in different microorganisms isolated from habitats exposed to these chemicals [4–8]. Here, novel pathways can evolve as a result of sufficient positive selective pressure for either the detoxification of such chemicals or their use as a new nutrient source [2]. Typically, novel degradation pathways emerge in a process called patchwork assembly by the recruitment, adaptation, and mutation of one or more genes encoding promiscuous enzymes from other metabolic pathways, either from within the host organism via gene duplication or via horizonal gene transfer (HGT) from the microbial community [1, 2, 9]. If the mutations happen to increase the substrate affinity and catalytic activity towards the respective new substrate and if the new catalytic activity enables the host to transform the new substrate into metabolites of an already existing metabolic pathway, it will gain a selective advantage over competing microbes by being able to use this compound as a new nutrient and energy resource [1, 2]. The genetic information encoding such novel catabolic pathways is often located on mobile genetic elements, such as plasmids or transposons, enabling transfer of the novel pathway to other microbes via HGT [4, 10, 11]. Eventually, positive selection for the new catabolic trait can lead to a loss of mobility and manifestation of the new pathway in the genome of its host.

However, the environmental concentrations of synthetic compounds may be too low to provide enough selection pressure for the evolution of novel catabolic pathways. Especially in wastewater treatment plants where the availability of other, readily degradable organic

compounds is high, many low-concentrated synthetic compounds presumably reside too shortly for the evolution of novel degradation pathways and remain in the purified wastewater as so-called micropollutants [12, 13]. Even some synthetic and natural compounds for which efficient biodegradation pathways exist, such as steroid hormones, are sometimes not fully metabolized in wastewater treatment plants due to their low concentration and contribute to the micropollutant pool. To enhance the biodegradation of such micropollutants, bioaugmentation of water treatment facilities is increasingly being considered, which implies the establishment of microorganisms in the water purification processes, which have been isolated for their ability to efficiently degrade the respective organic compounds [14, 15].

The study presented here was originally set up to isolate bacteria capable of degrading steroid hormones in low concentrations from activated sludge. To increase the chances of isolating strains that can later be established for bioaugmentation in real wastewater treatment plant conditions, we used an artificial wastewater medium to mimic typical wastewater nutrient conditions. Surprisingly, our enrichment procedure resulted in the isolation of a bacterial strain that did not grow with the provided steroid hormones, but with the synthetic medium buffer TRIS (2-amino-2-(hydroxymethyl)propane-1,3-diol). Herein, we pursued this finding further and present the identification and characterization of a bacterial degradation pathway for TRIS, which has been considered to be biologically inert so far.

76 # Results

77 ## Isolation and characterization of the TRIS-degrading strain *Pseudomonas hunanensis* Teo1

78 The first TRIS-degrading organism was isolated from an enrichment culture that was
79 originally designed to isolate testosterone-degrading bacteria from activated sludge (**Supp.**
80 **Methods**). We repeatedly observed growth in the enrichment cultures in TRIS-buffered
81 artificial wastewater medium without removal of the provided carbon source testosterone (not
82 shown). Plating of the enrichment cultures onto solid medium containing testosterone resulted
83 in the isolation of a bacterial strain that was not able to grow with testosterone but showed
84 growth in liquid artificial wastewater medium without the addition of any extra carbon or
85 nitrogen source. Subsequent growth experiments in phosphate buffered minimal medium with
86 different concentrations of TRIS confirmed a linear relationship between the provided TRIS
87 concentration and the amount of biomass produced by the isolate (**Fig. 1A**), suggesting that
88 TRIS was the growth substrate in these cultures. Growth experiments coupled with HPLC-MS
89 analysis confirmed that TRIS was completely removed from the culture medium, suggesting
90 its utilization as a carbon and nitrogen source for growth (**Fig. 1B-D**). The isolate had an
91 exponential growth rate of 0.36 +/- 0.09 h^{-1} and a doubling time of 0.44 +/- 0.09 h (n = 6). The
92 only detectable metabolite accumulating in the medium was ammonium, with around 40 % of
93 the nitrogen introduced with the TRIS substrate being released as ammonium into the medium
94 (**Fig. 1C-D**). The strain did not grow with the structurally similar amino alcohols serinol, 2-
95 amino-2-methyl-1-propanol, and 2-amino-2-methyl-1,3-propanediol (**Supp. Fig. S1**), while it
96 did grow with the quaternary ammonium compounds choline and betaine, and the secondary
97 amine sarcosine, and with the amino acids D- and L-serine, but not with glycine. Based on its
98 whole genome sequence (**Supp. Methods**), the isolate was taxonomically classified as a
99 representative of the species *Pseudomonas hunanensis* and was named strain Teo1 (**Supp. Tab.**
100 **ST1**). The genome of strain Teo1 consists of a circular chromosome (6.13 Mbp) and two large,
101 circular plasmids, p1_Teo1 (156.3 kbp) and p2_Teo1 (65.0 kbp).

102 ## Identification of TRIS degradation genes

103 TRIS growth experiments and time-resolved analysis of TRIS degradation in cell
104 suspensions of strain Teo1 showed that Tris degradation was induced in cells pre-grown with
105 TRIS while it was not induced in pyruvate pre-grown cells (**Supp. Fig. S2**), suggesting that
106 TRIS catabolism is regulated at the transcriptional level in strain Teo1. Based on this
107 observation we used transcriptomics of TRIS-grown and pyruvate-grown Teo1 cells to identify

108 potential TRIS degradation genes. A total of 398 genes were differentially regulated in TRIS-
109 compared to pyruvate-grown cells (fold change (FC) > 4, $p_{adj} < 0.05$, **Fig. 1E**, **Dataset SD1**),
110 of which 65 were upregulated in TRIS-grown cells. Ten of the twelve most upregulated genes
111 in TRIS-grown cells were found in two adjacent gene clusters (**Fig. 1E-G**) localized on the
112 p1_Teo1 plasmid. The proteins encoded in cluster I were annotated as a solute binding protein,
113 an amino acid/polyamine transporter, a choline dehydrogenase, a NAD/NADP-dependent
114 aldehyde dehydrogenase, a Δ(1)-pyrroline-2-carboxylate/Δ(1)-piperideine-2-carboxylate
115 reductase, and an alpha-ketoglutaric semialdehyde dehydrogenase (**Tab. 1**). The proteins
116 encoded in cluster II were annotated as a serine hydroxymethyltransferase, a D-serine
117 dehydratase, and two proteins presumably involved in the transformation of methylene
118 tetrahydrofolate into tetrahydrofolate and formate. The clusters are separated by a gene that
119 encodes a helix-turn-helix (HTH)-type transcriptional regulator. Based on the similar
120 upregulation of their genes, both gene clusters appear to be expressed as operons (**Fig. 1G**).
121 Due to their strong upregulation and their colocalization in putative operons we proposed that
122 these genes or a subset of them are involved in TRIS degradation in strain Teo1.

123 Characterization of the initial TRIS degradation reactions

124 Based on the predicted protein functions encoded in the upregulated gene clusters, we
125 hypothesized that TRIS is initially oxidized by the proteins encoded in cluster I. To test this,
126 we cloned combinations of the genes encoding the putrescine importer-like protein, the choline
127 dehydrogenase-like protein and the aldehyde dehydrogenase into the expression plasmid
128 pUCp18 into *E. coli* (**Suppl. Methods**) and tested high density cell suspensions of the resulting
129 strains for TRIS transformation activity. While the *E. coli* strains that carry only the putrescine
130 importer gene or the choline and aldehyde dehydrogenase genes did not transform TRIS, the
131 strain with all three genes transformed TRIS almost completely into a new compound within
132 24 h (**Fig. 2A**). This compound was identified as 2-hydroxymethylserine (**Fig. 2B**) based on
133 its molecular weight, which was 14 Da heavier than that of TRIS, suggesting the oxidation of
134 one hydroxymethyl group into a carboxylic group. To test whether this presumable TRIS
135 degradation intermediate can be further utilized by strain Teo1, sterilized culture supernatants
136 containing 2-hydroxymethylserine were used as growth medium for Teo1, confirming that
137 strain Teo1 can grow with and fully degrade 2-hydroxymethylserine (**Fig. 2C**). These results
138 supported our hypothesis that TRIS is transported into the cells by the putrescine importer-like
139 protein and subsequently oxidized by the choline dehydrogenase-like protein and the aldehyde
140 dehydrogenase. Thus, we propose that these genes encode a TRIS uptake protein (TupA), and

141 two TRIS-oxidizing proteins, namely a TRIS alcohol dehydrogenase (TaoA) and a TRIS
142 aldehyde dehydrogenase (TaoB).

143 Isolation of further TRIS-degrading bacteria and genomic analysis of TRIS degradation

144 Subsequent targeted enrichment of TRIS-degrading bacteria resulted in the isolation of
145 seven *Pseudomonas* strains (Teo2, Teo3, Teo4, Teo6, Teo8, Teo10, and Teo11) and one
146 *Shinella zoogloeoides* strain (Teo12) (**Supp. Tab. ST1**). All isolates were all able to grow with
147 TRIS as only carbon and nitrogen source and completely removed TRIS from the culture
148 medium (**Supp. Fig. S3**). The *Pseudomonas* strains Teo2, Teo4, Teo6, Teo8, and Teo11 and
149 the *Shinella* isolate strain Teo12 were isolated from different municipal wastewater treatment
150 plant samples, *Pseudomonas sichuanensis* Teo3 from an activated charcoal basin of a water
151 purification plant, and *Pseudomonas* sp. strain Teo10 from a freshwater lake sample.
152 Enrichment cultures from two additional wastewater treatment plants and from five freshwater
153 habitats did not develop growth (**Supp. Tab. ST1)**.

154 We sequenced the genomes of five *Pseudomonas* isolates (**Supp. Methods**) and found
155 homologous TRIS degradation gene clusters to the ones identified in strain Teo1 in all of these
156 strains (**Fig. 3, Suppl. Fig. S4**). In *Pseudomonas* strains Teo2, Teo4, Teo6, and Teo8 the
157 clusters are also localized on plasmids (p1_Teo2, p1_Teo4, p1_Teo6, and p2_Teo8) and the
158 plasmids have high similarities to p1_Teo1 (**Fig. 3A**). In *Pseudomonas* strain Teo3, the clusters
159 are encoded in the chromosome (**Fig. 3B**). While all gene clusters II are highly similar, only
160 the *tupA*, *taoA*, and *taoB* genes are conserved in all cluster I sequences (**Fig. 3, Suppl. Fig. S4**),
161 suggesting that the Δ(1)-pyrroline-2-carboxylate/Δ(1)-piperideine-2-carboxylate reductase-
162 like protein and the alpha-ketoglutaric semialdehyde dehydrogenase-like protein are not
163 required for TRIS degradation. In all these strains, the TRIS degradation gene clusters are
164 flanked by sequences similar to known bacterial insertion elements (**Fig. 3B**), suggesting that
165 the TRIS degradation gene clusters are located within a mobile genetic element [11]. A search
166 in the NCBI nucleotide database identified one *Priestia* genome (accession CP065422.1) and
167 three *Pseudomonas* genomes (CP069081.1, CP097105.1, CP114115.1) with homologous gene
168 clusters **(Fig. 3A, Suppl. Fig. S4)**. In *Priestia*, and two of the *Pseudomonas* strains the clusters
169 are also plasmid-borne, while they are encoded chromosomally in *Pseudomonas* sp. strain
170 GXZC (**Fig. 3B**).

171 We also sequenced the genome of the *Shinella* isolate (**Supp. Methods**), which consists of
172 one circular chromosomes (3.54 Mbp) and three circular plasmids, p1_Teo12 (1.89 Mbp),
173 p2_Teo12 (221.54 kbp) and p3_Teo12 (140.01 kbp), which have no apparent similarity to the

174 TRIS degradation-encoding *Pseudomonas* plasmids. However, a DNA region on p2_Teo12
175 encodes homologs of all TRIS degradation genes in two adjacent gene clusters, except for the
176 genes encoding the solute binding protein, the uptake protein TupA, the Δ(1)-pyrroline-2-
177 carboxylate/Δ(1)-piperideine-2-carboxylate reductase-like protein, and the alpha-ketoglutaric
178 semialdehyde dehydrogenase-like protein (**Fig. 3B, Suppl. Fig. S4**). In these clusters, the *taoA*
179 and *taoB* gene homologs are encoded in the same orientation as in cluster I of the *Pseudomonas*
180 TRIS degradation gene clusters, while the genes are differently oriented in cluster II. A
181 homologous regulator gene to the one found in the *Pseudomonas* gene clusters is located
182 upstream of this cluster. A search in the NCBI nucleotide database identified a closely related
183 *Rhizobium oryzihabitans* strain M15 (CP048637.1), that carries a homologous DNA segment
184 on a plasmid (p5, **Fig. 3B**). The predicted TRIS degradation gene clusters in *S. zoogloeoides*
185 *Teo12* and strain M15 are separated by a truncated transposase gene and flanked by additional
186 transposase genes and insertion elements.
187 A phylogenetic analysis of the TaoA proteins with closely related proteins of the glucose-
188 methanol-choline oxidoreductase family (GMC, InterPro IPR012132) revealed that the TaoA
189 proteins form a unique cluster that diverges from a clade containing choline dehydrogenase
190 protein sequences (**Supp. Fig. S5A**). In contrast, other choline dehydrogenase proteins of the
191 TRIS-degrading isolates encoded outside of the TRIS degradation gene clusters cluster within
192 the choline dehydrogenase clade, except for two choline dehydrogenase proteins from *S.*
193 *zoogloeoides Teo12*, which cluster at the base of the TaoA cluster. A phylogenetic analysis of
194 the TaoB proteins with closely related proteins containing an aldehyde dehydrogenase domain
195 (InterPro IPR015590**)** showed that the TaoB proteins also from a distinct cluster within the
196 dataset with closest relations to a reviewed aldehyde dehydrogenase (PuuC, Accession P23882)
197 that oxidizes aldehydes during putrescine catabolism in *E. coli* (**Supp. Fig. S5B**). Other PuuC-
198 like proteins encoded outside of the TRIS degradation gene clusters of the TRIS-degrading
199 isolates cluster in close proximity to the TaoB cluster.

200 Conjugational transfer of TRIS degradation plasmids

201 The TRIS degradation-encoding *Pseudomonas* plasmids have high similarities to the
202 previously described large plasmids pND6-2 from *Pseudomonas putida* ND6 and pS04-90
203 from *Pseudomonas aeruginosa* S04-90 [16, 17]. Both these plasmids lack the putative mobile
204 genetic element that encodes TRIS degradation (**Fig. 3A, Suppl. Fig. S4**). However, pS04-90
205 carries a carbapenem resistance-encoding class 1 integron at almost the same site in the pND6-
206 2 backbone as the TRIS degradation-encoding elements in the *Pseudomonas* plasmids. Both

pND6-2 and pS04-90 are conjugative plasmids that can be transferred from their hosts into other *Pseudomonas* strains. Like pND6-2 and pS04-90, p1_Teo1 and its homologs carry genes encoding type IV pili and a type IVB secretion system (**Fig. 3A, Suppl. Fig. S4**), suggesting that these plasmids are also conjugative plasmids. To test this, we set up conjugation experiments with strain Teo1 and strain Teo8 as plasmid donors and *Pseudomonas putida* KT2440 as a non-TRIS-degrading recipient. To be able to differentiate between donor and recipient cells, we labelled strain KT2440 with a chromosomally integrated gentamycin resistance associated with a yellow fluorescent protein (YFP) gene. After the conjugation of Teo1 and Teo8 with strain KT2440::*eyfp-gm* growth of fluorescing colonies was observed on gentamycin-containing minimal medium plates with TRIS as only carbon and nitrogen source (**Fig. 4A**), suggesting that conjugational transfer of the p1_Teo1 and p2_Teo8 plasmids also transferred the ability to use TRIS as growth substrate to KT2440::*eyfp-gm*. The resulting transconjugants were also able to grow with TRIS in liquid culture (**Fig. 4D**), confirming that both gene clusters together encode the complete degradation pathway sufficient to use TRIS as sole carbon and nitrogen source.

224 ## Discussion

225 In this study we identify and characterize a degradation pathway for the synthetic buffer
226 compound TRIS in several *Pseudomonas* strains and a *Shinella* strain, which were all isolated
227 from wastewater purification systems with TRIS as only carbon source. Our results suggest
228 that TRIS degradation proceeds via a pathway that originated recently via a combination of
229 genes from different, formerly independent metabolic pathways and their assembly into two
230 co-regulated gene clusters within a mobile genetic element. Although not all individual
231 functions for the proteins encoded in clusters I and II were biochemically confirmed,
232 conjugational transfer of the plasmid that contains both clusters into *P. putida* KT2440 co-
233 transferred the ability to degrade TRIS, confirming that they together encode the complete
234 degradation pathway sufficient to use TRIS as sole carbon and nitrogen source.

235 TRIS has long been considered biologically inert, because the bonding of its amino
236 group to a tertiary carbon atom prevents its metabolism via transamination or oxidative
237 deamination, which are the most common reactions in the degradation of amines. However,
238 bacterial degradation of α-amino acids with a tertiary α-carbon atom is known for a long time
239 and has been demonstrated for 2-hydroxymethylserine via a tetrahydrofolate-dependent
240 methylserine hydroxymethyltransferase (mSHMT) with D-serine and formaldehyde as
241 products [18]. All of our TRIS-degrading isolates encode a protein in cluster II with highest
242 similarities to confirmed D-amino acid-producing mSHMTs [19] as well as a protein for the
243 degradation of D-serine to pyruvate, suggesting that these proteins together can catalyze the
244 degradation of 2-hydroxymethylserine, the product of TRIS oxidation by the TaoAB proteins.
245 Thus, we propose a pathway for the catabolism of TRIS, in which TRIS is translocated into the
246 cytoplasm by the TRIS uptake protein TupA and subsequently oxidized to 2-
247 hydroxymethylserine by the TRIS alcohol dehydrogenase TaoA and the TRIS aldehyde
248 dehydrogenase TaoB via a suspected aldehyde intermediate (**Fig. 5**). 2-Hydroxymethylserine
249 is further transformed into D-serine by the mSHMT protein, which is then transformed into
250 pyruvate by the D-serine dehydratase. The latter can be channelled into the tricarboxylic acid
251 cycle via oxidative decarboxylation to acetyl-CoA. The formaldehyde-accepting
252 tetrahydrofolate (THF) cofactor of the mSHMT protein can then be recycled by the
253 bifunctional methylenetetrahydrofolate dehydrogenase/ methenyltetrahydrofolate
254 cyclohydrolase FolD and the formyltetrahydrofolate deformylase PurU encoded in cluster II
255 [20, 21].

256 The genetic context of the *tupA*, *taoA* and *taoB* genes is not found outside of cluster I,
257 suggesting that these genes were assembled from multiple origins. The TaoA proteins have
258 highest similarities to choline dehydrogenases (CDH), which catalyse the oxidation of choline
259 into betaine aldehyde [22] and belong to the glucose-methanol-choline oxidoreductase family
260 (GMC). Within a phylogenetic GMC protein tree, the TaoA proteins form a distinct clade that
261 diverges from the CDH sequences with strong bootstrap support, suggesting that the TRIS
262 alcohol dehydrogenase functionality evolved from enzymes with choline dehydrogenase
263 activity. Strikingly, two CDH proteins encoded outside of gene cluster I in *S. zoogloeoides*
264 Teo12 cluster basal to the TaoA protein clade, suggesting that they could be ancestral to TaoA.
265 It is tempting to speculate that the TaoA proteins have originated in *Shinella* or a similar
266 organism through the duplication and mutation of CDH-encoding genes. TupA and TaoB have
267 highest similarities to proteins involved in the degradation of polyamines like putrescine [23,
268 24], suggesting that these proteins were recruited from bacterial polyamine degradation
269 pathways [25]. The fact that Teo1 was not able to use other α-substituted amino alcohols such
270 as 2-amino-2-methylpropanol and 2-amino-2-methylproandiol as growth substrates suggests
271 that either the substrate uptake by TupA or the oxidation reactions catalysed by TaoAB evolved
272 to be highly specific for TRIS.
273 Expression of *tupA* was strictly required for TRIS transformation in *E. coli* cells,
274 suggesting that TRIS translocation is required for TRIS uptake in Gram-negative cells. With a
275 pKa of 8.07 TRIS is mainly positively charged at neutral and acidic pH, preventing its diffusion
276 across the cytoplasmic membrane. The absence of a *tupA* gene homolog in *S. zoogloeoides*
277 Teo12 suggests that this gene was recruited later to the pathway. It remains unknow how TRIS
278 is translocated by Teo12, however, alternative putrescine uptake transporters [23] are also
279 encoded in the genome of Teo12, which might play a role in TRIS uptake in this strain.
280 The genetic context of the genes encoded in cluster II is also present in other
281 *Pseudomonas* strains that do not encode cluster I, suggesting that this gene cluster may have
282 been assembled prior to its recruitment into the TRIS degradation pathway. While SHMT and
283 mSHMT proteins are often accompanied by THF co-factor recycling proteins [19, 26], their
284 genetic association with D-amino acid degradation genes such as the D-serine dehydratase
285 genes in cluster II in a putative operon was not reported so far. In pathogenic bacteria, D-serine
286 dehydratase genes play important roles in the detoxification and catabolism of D-amino acids
287 [27, 28]. Thus, we conclude that the second part of the TRIS degradation pathway was
288 assembled by a combination of genes involved in the transformation of α-substituted amino
289 acids and in the degradation of D-amino acids. The presence of mostly incomplete insertion

290 elements up- and downstream of the TRIS degradation gene clusters suggests that the whole
291 DNA segment was originally able to be mobilized as a composite transposon, allowing its
292 transposition between plasmids and the chromosome. The finding of an additional transposase
293 gene between the two gene clusters in *Shinella* and the closely related *Rhizobium* strain
294 corroborates our hypothesis that the pathway was assembled from two independent reactions
295 sequences encoded in clusters I and II.

296 TRIS is used in countless applications in research, industry, medicine, and household
297 settings. Its most prominent applications include its use as a buffer in molecular biology and
298 biochemistry labs, as an excipient in drug formulations, and as an active agent for the treatment
299 of metabolic acidosis and an enhancer for antibiotics and antiseptics for the treatment of Gram-
300 negative infections. Based on its first large scale production in the middle of the twentieth
301 century [29, 30], we hypothesize that the TRIS degradation pathway evolved within the last
302 thirty to fifty years, which is corroborated by the fact that TRIS degradation was not discovered
303 earlier despite its intense use in research laboratories. However, the organization of the TRIS
304 degradation genes in two compact gene clusters and the fact that expression of these
305 presumable operons was regulated in response to TRIS in strain Teo1 are signs for a highly
306 evolved pathway [5], suggesting its turn-around in the environment for a while. The regulator
307 gene between the two clusters is presumably involved in this regulation. Its protein product is
308 similar to the transcription factor GltC that regulates glutamate synthase expression in *Bacillus*
309 *subtilis* [31]. The first reports of bacteria being able to utilize TRIS as a growth substrate were
310 published thirty years ago from a group in Spain [32], however, no genetic or biochemical
311 analyses followed this observation.

312 Specific microbial habitats such as sinks and wastewater treatment facilities of large
313 research laboratories, hospitals, or from the TRIS-manufacturing industry could be locations
314 where the TRIS degradation pathway might have originated. First, such habitats encounter
315 significant TRIS concentrations on a regular basis. For example, the antibiotic fosfomycin,
316 which is produced and administered as a TRIS salt, was found at concentrations of 0.13 mM
317 in the influent and 0.015 mM in the effluent of a wastewater treatment plant of a fosfomycin
318 production plant [33], suggesting the presence of similar concentrations of its counterion TRIS.
319 Second, sinks and water purification systems are hotspots for horizontal gene transfer (HGT)
320 [11, 34, 35], which additionally favors the evolution of novel catabolic pathways.

321 The identification of identical TRIS degradation gene clusters in bacteria that have been
322 isolated in Germany, the Republic of Korea, and in China corroborates our findings, that TRIS
323 degradation-encoding plasmids can be readily transferred among bacteria by conjugation-

driven HGT. Our isolation studies suggest that the TRIS degradation pathway is frequently present in the microbiome of municipal wastewater treatment plants but less frequent in freshwater habitats, indicating that environments with high carbon and nitrogen loads better support the maintenance and dissemination of the TRIS degradation pathway than more oligotrophic environments. Although the average TRIS concentration in the sampled wastewater treatment plants is presumably very low, its metabolism as an additional nitrogen and carbon source alongside other recalcitrant molecules might provide sufficient positive selection pressure for bacteria with broad substrate ranges such as *Pseudomonas* and *Shinella* [36–39] to maintain the pathway. Our results corroborate the importance of HGT and mobile genetic elements in the evolution of novel catabolic pathways. With this, they provide additional knowledge about the basic structure of such elements, which can be used for future use in engineering bacteria for bioaugmentation [11].

337 # Experimental procedures

338 Additional experimental methods can be found in the supplemental information.

339 ## Targeted enrichment and growth cultures

340 TRIS-degrading strains were isolated and grown in a phosphate-buffered minimal medium (pH
341 7.0) containing 0.01 mM $CaCl_2$ x 2 H_2O, 1.5 mM $MgSO_4$ x 7 H_2O, 35 mM K_2HPO_4 x 3 H_2O,
342 15 mM NaH_2PO_4 x H_2O, trace elements and 10 mM TRIS. For solid media plates, 1.5 % agar
343 was added prior to autoclaving. Enrichment cultures (5 ml) were inoculated with fresh samples
344 (1 ml) from local wastewater treatment plants (activated sludge or activated carbon), a water
345 purification plant (activated carbon), or different freshwater habitats (**Supp. Tab. ST1**). When
346 enrichment cultures showed growth, 100 µl of the culture supernatant were transferred to 5 ml
347 fresh minimal medium with TRIS, and this was repeated two to three times before cultures
348 were spread onto solid minimal medium plates containing to isolate individual TRIS-degrading
349 colonies. Growth experiments in liquid cultures were carried out at 30°C and 200 rpm in 1 ml
350 or 5 ml medium in 24-well plates or in reaction tubes, respectively. Experimental cultures were
351 inoculated from washed, over-night starter cultures grown with TRIS. Growth was followed
352 by measuring the optical density at 600 nm (OD_{600}). For transcriptome experiments, TRIS was
353 replaced with 20 mM pyruvate and 20 mM NH_4Cl were added as nitrogen source. For substrate
354 tests, TRIS was replaced with 10 mM D- or L-serine, 10 mM choline, 10 mM betaine, 10 mM
355 2-amino-2-methylpropanol, 10 mM 2-amino-2-methylproandiol, 10 mM sarcosine, or 10 mM
356 serinol, and 20 mM NH_4Cl were added as nitrogen source. *Pseudomonas putida* KT2440 and
357 its derivatives were grown in the same minimal medium with succinate as carbon source at
358 30°C. *E. coli* strains were grown in half-concentrated lysogeny broth (LB) at 37°C. If required,
359 kanamycin (20-50 µg/ml), tetracycline (10 µg/ml), or gentamycin (20-40 µg/ml) antibiotics
360 were added to the medium after autoclaving. To test whether 2-hydroxymethylserine can be
361 used as a growth for Teo1, cell suspensions of *tupA*, *taoB* and *taoA* expressing *E. coli* cells that
362 had produced 2-hydroxymethylserine from TRIS were centrifuged and sterile filtered (0.2 µm)
363 and the culture supernatant was inoculated with strain Teo1 cells.

364 ## TRIS quantification

365 TRIS, its degradation intermediates, and ammonium were identified and quantified by high
366 performance liquid chromatography (HPLC) coupled to a mass spectrometer and a UV/Vis
367 detector [40] after derivatization of their amino group with diethyl ethoxymethylenemalonate
368 (DEEMM, [41]). For this, 100 µl culture supernatants were mixed with 130 µl borate buffer (1

369 M, pH 9.0), 75 µl methanol, and 3 µl DEEM reagent, followed by 30 min sonication and 60
370 min incubation at 70°C before injection into the HPLC. A gradient (flow rate 0.3 ml/min) of
371 ammonium-acetate buffer (10 mM, pH 3.0, with 0.1 % (v/v) formic acid, eluent A) and
372 acetonitrile (eluent B) were used for product elution starting with 10 % eluent B for 2 min,
373 increasing to 90 % eluent B within 22 min, remaining at 90 % eluent B for 2 min, and returning
374 to 10 % eluent B within 1 min, followed by an equilibration of 5 min. Products were identified
375 based on their mass spectra after electrospray ionization in positive ion mode. The capillary
376 voltage was 2500 V, the end plate offset 500 V and the capillary temperature 300°C. Nebulizer
377 pressure was 22.5 psi, dry gas flow 12 l/min and dry temperature 200°C. Quantification was
378 performed based on the product peak areas at 280 nm UV absorbance, and concentrations were
379 calculated based on concentration curves of authentic standards treated in the same way. The
380 concentration of 2-hydroxymethylserine was calculated using the same standard curve as for
381 TRIS.

382 Transcriptome analysis

383 *P. hunanensis* Teo1 was grown in minimal medium with TRIS as only carbon and nitrogen
384 source or with pyruvate and ammonium and cultures were harvested during mid-log phase.
385 Harvested cells were re-suspended in 800 µl RLT buffer (RNeasy Mini Kit, Qiagen) with β-
386 mercaptoethanol (10 µl ml^{-1}) and cell lysis was performed using a laboratory ball mill.
387 Subsequently, 400 µl RLT buffer (RNeasy Mini Kit Qiagen) with β-mercaptoethanol (10 µl
388 ml^{-1}) and 1200 µl 96% (vol./vol.) ethanol were added. For RNA isolation, the RNeasy Mini Kit
389 (Qiagen) was used as recommended by the manufacturer, but instead of RW1 buffer RWT
390 buffer (Qiagen) was used in order to isolate RNAs smaller than 200 nucleotides also. For
391 sequencing, the strand-specific cDNA libraries were constructed with a NEB Next Ultra II
392 Directional RNA library preparation kit for Illumina and the NEB Next Multiplex Oligos for
393 Illumina (New England BioLabs, Frankfurt am Main, Germany). Sequencing was performed
394 by using the HiSeq2500 instrument (Illumina Inc., San Diego, CA, USA) using the HiSeq
395 Rapid SR Cluster Kit v2 for cluster generation and the HiSeq Raid SBS Kit (50 cycles) for
396 sequencing in the single-end mode and running 1x50 cycles. Raw reads have been deposited
397 in the Sequence Read Archive under study SRP451968 (SRR25447477-SRR25447482). More
398 detailed information can be found in the Supplementary Information.

399 Conjugation experiments

400 Conjugation experiments were carried out using strains Teo1 and Teo8 as donors and
401 gentamicin-resistant *P. putida* KT2440::*eyfp-gm* as recipient. Approximately 1 x 10^9 donor
402 cells and 3 x 10^9 recipient cells were mixed and spotted onto sterile cellulose acetate filter disks
403 (ca. 3 cm^2, 0.45 µm pores) on LB agar plates. Conjugation plates were incubated at 30°C for
404 24 h before cells were washed off the filter disks with 50 mM phosphate buffer (pH 7.2).
405 Decimal dilutions were plated onto minimal medium agar plates with TRIS as only carbon and
406 nitrogen source containing 40 µg/ml gentamicin. Transconjugants were screen using a
407 ChemiDocTM Imaging System (Bio-Rad) using blue epi illumination and an emission filter at
408 530 nm. The conjugation rate was calculated by dividing the number of positive
409 transconjugants by the number of recipient cells in each assay. The successful transfer of the
410 p1_Teo1 and p2_Teo8 plasmids was confirmed by colony PCR amplifying the *tupA*, *taoA*,
411 *taoB*, *glyA*, and *dsdA* genes (**Suppl. Tab. ST2**).
412

Acknowledgment

The authors thank the operators and the employers of the water treatment facilities in the cities of Münster, Hamm, Dülmen, and Güthersloh-Putzhagen for their help with sampling. We especially thank Rudolf Cigelski (Hamm) for his continued support and his great efforts to provide us with samples. We further thank Malte Jochimsen, Anna Hannes, and David Wallbraun for experimental support.

Competing Interest Statement

The authors declare no conflict of interest.

Data availability

The whole-genome shotgun projects have been deposited at DDBJ/ENA/GenBank under the BioProject accession numbers PRJNA999090, PRJNA999091, PRJNA999092, PRJNA999094, PRJNA999097, PRJNA999137, PRJNA999141 and the transcriptome data under the BioProject accession number PRJNA999090 with the SRA accession numbers SRR25447477 - SRR25447482.

428 ## References

429

430 1. Kolvenbach BA, Helbling DE, Kohler H-PE, Corvini PF-X. Emerging chemicals and the
431 evolution of biodegradation capacities and pathways in bacteria. *Curr Opin Biotechnol*
432 2014; **27**: 8–14.

433 2. Copley SD. Evolution of efficient pathways for degradation of anthropogenic chemicals.
434 *Nat Chem Biol* 2009; **5**: 559–566.

435 3. Udiković-Kolić N, Scott C, Martin-Laurent F. Evolution of atrazine-degrading capabilities
436 in the environment. *Appl Microbiol Biotechnol* 2012; **96**: 1175–1189.

437 4. Top EM, Springael D, Boon N. Catabolic mobile genetic elements and their potential use
438 in bioaugmentation of polluted soils and waters. *FEMS Microbiol Ecol* 2002; **42**: 199–
439 208.

440 5. Johnson GR, Spain JC. Evolution of catabolic pathways for synthetic compounds: bacterial
441 pathways for degradation of 2,4-dinitrotoluene and nitrobenzene. *Appl Microbiol*
442 *Biotechnol* 2003; **62**: 110–123.

443 6. Aulestia M, Flores A, Acosta-Jurado S, Santero E, Camacho EM. Genetic characterization
444 of the ibuprofen-degradative pathway of *Rhizorhabdus wittichii* MPO218. *Appl Environ*
445 *Microbiol* 2022; **88**: e00388-22.

446 7. Bonatelli ML, Rohwerder T, Popp D, Liu Y, Akay C, Schultz C, et al. Recently evolved
447 combination of unique sulfatase and amidase genes enables bacterial degradation of the
448 wastewater micropollutant acesulfame worldwide. *Front Microbiol* 2023; **14**:
449 14:1223838.

450 8. Rios-Miguel AB, Smith GJ, Cremers G, Van Alen T, Jetten MSM, Op Den Camp HJM, et
451 al. Microbial paracetamol degradation involves a high diversity of novel amidase enzyme
452 candidates. *Water Res X* 2022; **16**: 100152.

453 9. Copley SD. Evolution of a metabolic pathway for degradation of a toxic xenobiotic: the
454 patchwork approach. *Trends Biochem Sci* 2000; **25**: 261–265.

455 10. Springael D, Top EM. Horizontal gene transfer and microbial adaptation to xenobiotics:
456 new types of mobile genetic elements and lessons from ecological studies. *Trends*
457 *Microbiol* 2004; **12**: 53–58.

458 11. Rios Miguel AB, Jetten MSM, Welte CU. The role of mobile genetic elements in organic
459 micropollutant degradation during biological wastewater treatment. *Water Res X* 2020; **9**:
460 100065.

461 12. Schwarzenbach RP, Escher BI, Fenner K, Hofstetter TB, Johnson CA, von Gunten U, et
462 al. The challenge of micropollutants in aquatic systems. *Science* 2006; **313**: 1072–1077.

463 13. Petrie B, Barden R, Kasprzyk-Hordern B. A review on emerging contaminants in
464 wastewaters and the environment: Current knowledge, understudied areas and
465 recommendations for future monitoring. *Water Res* 2015; **72**: 3–27.

466 14. Benner J, Helbling DE, Kohler H-PE, Wittebol J, Kaiser E, Prasse C, et al. Is biological
467 treatment a viable alternative for micropollutant removal in drinking water treatment
468 processes? *Water Res* 2013; **47**: 5955–5976.

469 15. Herrero M, Stuckey DC. Bioaugmentation and its application in wastewater treatment: A
470 review. *Chemosphere* 2015; **140**: 119–128.

471 16. van der Zee A, Kraak WB, Burggraaf A, Goessens WHF, Pirovano W, Ossewaarde JM, et
472 al. Spread of carbapenem resistance by transposition and conjugation among
473 *Pseudomonas aeruginosa*. *Front Microbiol* 2018; **9**: 2057.

474 17. Wang S, Li S, Du D, Wang D, Yan W. Conjugative transfer of megaplasmids pND6–1 and
475 pND6–2 enhancing naphthalene degradation in aqueous environment: characterization
476 and bioaugmentation prospects. *Appl Microbiol Biotechnol* 2020; **104**: 861–871.

477 18. Wilson EM, Snell EE. Metabolism of α-methylserine. *J Biol Chem* 1962; **237**: 3171–3179.

478 19. Nozaki H, Kuroda S, Watanabe K, Yokozeki K. Cloning of the gene encoding α-
479 methylserine hydroxymethyltransferase from *Aminobacter* sp. AJ110403 and *Ensifer* sp.
480 AJ110404 and characterization of the recombinant enzyme. *Biosci Biotechnol Biochem*
481 2008; **72**: 3002–3005.

482 20. D'Ari L, Rabinowitz JC. Purification, characterization, cloning, and amino acid sequence
483 of the bifunctional enzyme 5,10-methylenetetrahydrofolate dehydrogenase/5,10-
484 methenyltetrahydrofolate cyclohydrolase from *Escherichia coli*. *J Biol Chem* 1991; **266**:
485 23953–23958.

486 21. Nagy PL, Marolewski A, Benkovic SJ, Zalkin H. Formyltetrahydrofolate hydrolase, a
487 regulatory enzyme that functions to balance pools of tetrahydrofolate and one-carbon
488 tetrahydrofolate adducts in *Escherichia coli*. *J Bacteriol* 1995; **177**: 1292–1298.

489 22. Wargo MJ. Homeostasis and catabolism of choline and glycine betaine: Lessons from
490 *Pseudomonas aeruginosa*. *Appl Environ Microbiol* 2013; **79**: 2112–2120.

491 23. Krysenko S, Wohlleben W. Polyamine and ethanolamine metabolism in bacteria as an
492 important component of nitrogen assimilation for survival and pathogenicity. *Med Sci*
493 2022; **10**: 40.

494 24. Luengo JM, Olivera ER. Catabolism of biogenic amines in *Pseudomonas* species. *Environ*
495 *Microbiol* 2020; **22**: 1174–1192.

496 25. Nemoto N, Kurihara S, Kitahara Y, Asada K, Kato K, Suzuki H. Mechanism for regulation
497 of the putrescine utilization pathway by the transcription factor PuuR in *Escherichia coli*
498 K-12. *J Bacteriol* 2012; **194**: 3437–3447.

499 26. Shetty S, Varshney U. Regulation of translation by one-carbon metabolism in bacteria and
500 eukaryotic organelles. *J Biol Chem* 2021; **296**: 100088.

501 27. Connolly JPR, Roe AJ. When and where? Pathogenic *Escherichia coli* differentially sense
502 host D-serine using a universal transporter system to monitor their environment. *Microb*
503 *Cell* 2016; **3**: 181–184.

504 28. Li G, Lu C-D. The cryptic *dsdA* gene encodes a functional D-serine dehydratase in
505 *Pseudomonas aeruginosa* PAO1. *Curr Microbiol* 2016; **72**: 788–794.

506 29. Bourguignon J, Sion M-X, Moreau M. Preparation of Tris(hydroxymethyl)aminomethane.
507 US Patent No. US4233245A, U.S. Patent and Trademark Office 1980.

508 30. McMillan GW. Electrolytic production of aminoalcohols. US Patent No. US2485982A,
509 U.S. Patent and Trademark Office 1949.

510 31. Bohannon DE, Sonenshein AL. Positive regulation of glutamate biosynthesis in *Bacillus*
511 *subtilis*. *J Bacteriol* 1989; **171**: 4718–4727.

512 32. Fábregas J, Vázquez V, Cabezas B, Otero A. Tris not only controls the pH in microalgal
513 cultures, but also feeds bacteria. *J Appl Phycol* 1993; **5**: 543–545.

514 33. Zeng P, Xie X, Song Y, Liu R, Zhu C, Galarneau A, et al. Ion chromatography as highly
515 suitable method for rapid and accurate determination of antibiotic fosfomycin in
516 pharmaceutical wastewater. *Water Sci Technol* 2014; **69**: 2014–2022.

517 34. Abe K, Nomura N, Suzuki S. Biofilms: hot spots of horizontal gene transfer (HGT) in
518 aquatic environments, with a focus on a new HGT mechanism. *FEMS Microbiol Ecol*
519 2020; **96**: fiaa031.

520 35. Diorio-Toth L, Wallace MA, Farnsworth CW, Wang B, Gul D, Kwon JH, et al. Intensive
521 care unit sinks are persistently colonized with multidrug resistant bacteria and
522 mobilizable, resistance-conferring plasmids. *mSystems* 2023; **8:** e00206-23.

523 36. Moore ERB, Tindall BJ, Martins Dos Santos VAP, Pieper DH, Ramos J-L, Palleroni NJ.
524 Nonmedical: Pseudomonas. In: Dworkin M, Falkow S, Rosenberg E, Schleifer K-H,
525 Stackebrandt E (eds). *The Prokaryotes*. 2006. Springer New York, New York, NY, pp
526 646–703.

527 37. Jiang HJ, Ma Y, Qiu GJ, Wu FL, Chen SL. Biodegradation of nicotine by a novel strain
528 *Shinella* sp. HZN1 isolated from activated sludge. *J Environ Sci Health Part B* 2011; **46**:
529 703–708.

530 38. Hesse C, Schulz F, Bull CT, Shaffer BT, Yan Q, Shapiro N, et al. Genome-based
531 evolutionary history of *Pseudomonas* spp. *Environ Microbiol* 2018; **20**: 2142–2159.

532 39. Huang Y, Yu Z, Liu L, Che Y, Zhang T. Acesulfame anoxic biodegradation coupled to
533 nitrate reduction by enriched consortia and isolated *Shinella* spp. *Environ Sci Technol*
534 2022; **56:** 13096-13106.

535 40. Holert J, Yücel O, Jagmann N, Prestel A, Möller HM, Philipp B. Identification of bypass
536 reactions leading to the formation of one central steroid degradation intermediate in
537 metabolism of different bile salts in *Pseudomonas* sp. strain Chol1. *Environ Microbiol*
538 2016; **8**: 3373–3389.

539 41. Alaiz M, Navarro JL, Girón J, Vioque E. Amino acid analysis by high-performance liquid
540 chromatography after derivatization with diethyl ethoxymethylenemalonate. *J*
541 *Chromatogr A* 1992; **591**: 181–186.

542

543

544 # Figure and table legends

545

546 **Tab. 1**: Genes potentially involved in TRIS degradation in *Pseudomonas hunanensis* Teo1.

Gene	Locus tag	Annotated function	Confirmed function and new gene ID	Protein family (InterProScan)	Best hit (Swiss-Prot)	% identity	
purU	PshuTeo1_56140	Formyltetrahydrofolate deformylase		Formyltetrahydrofolate deformylase (IPR004810)	Q46339, Formyltetrahydrofolate deformylase, *Corynebacterium* sp.	46.8	Cluster II
folD	PshuTeo1_56150	Bifunctional protein FolD		Tetrahydrofolate dehydrogenase/ cyclohydrolase (IPR000672)	A6UB98, Bifunctional protein FolD 2, *Sinorhizobium medicae*	73.0	Cluster II
dsdA	PshuTeo1_56160	D-serine dehydratase		D-serine ammonia-lyase (IPR011780)	B3PYT5, Probable D-serine dehydratase, *Rhizobium etli*	66.1	Cluster II
glyA	PshuTeo1_56170	Serine hydroxy-methyltransferase 2		Serine hydroxymethyltransferase (IPR001085)	B2DEU8, 2-methylserine hydroxymethyltransferase, *Aminobacter* sp.	66.6	Cluster II
gltC	PshuTeo1_56180	HTH-type transcriptional regulator		non predicted	P71318, Hydrogen peroxide-inducible genes activator, *Pectobacterium carotovorum*	26.9	
56190	PshuTeo1_56190	hypothetical protein		none predicted	P45766, Putative amino-acid ABC transporter-binding protein YhdW, *Escherichia coli*	68.9	Cluster I
puuP	PshuTeo1_56200	Putrescine importer	TRIS uptake protein, *tupA*	Amino acid/polyamine transporter I (IPR002293)	P76037, Putrescine importer PuuP, *Escherichia coli*	41.8	Cluster I
puuC	PshuTeo1_56210	NADP/NAD-dependent aldehyde dehydrogenase	TRIS aldehyde dehydrogenase, *taoB*	none predicted	P23883, NADP/NAD-dependent aldehyde dehydrogenase PuuC, *Escherichia coli*	46.0	Cluster I
betA	PshuTeo1_56220	Oxygen-dependent choline dehydrogenase	TRIS alcohol dehydrogenase, *taoA*	Glucose-methanol-choline oxidoreductase (IPR012132)	Q9L4K0, Oxygen-dependent choline dehydrogenase, *Chromohalobacter salexigens*	48.3	Cluster I
lhpD	PshuTeo1_56230	Δ(1)-Pyrroline-2-carboxylate/Δ(1)-piperideine-2-carboxylate reductase		Malate/L-lactate dehydrogenase-like (IPR003767)	Q9I492, Δ(1)-pyrroline-2-carboxylate/Δ(1)-piperideine-2-carboxylate reductase, *Pseudomonas aeruginosa*	67.0	Cluster I
aldH	PshuTeo1_56240	Alpha-ketoglutaric semialdehyde dehydrogenase		Alpha-ketoglutaric semialdehyde dehydrogenase (IPR044151)	Q6FFQ0, Alpha-ketoglutaric semialdehyde dehydrogenase, *Acinetobacter baylyi*	58.5	Cluster I

547

548

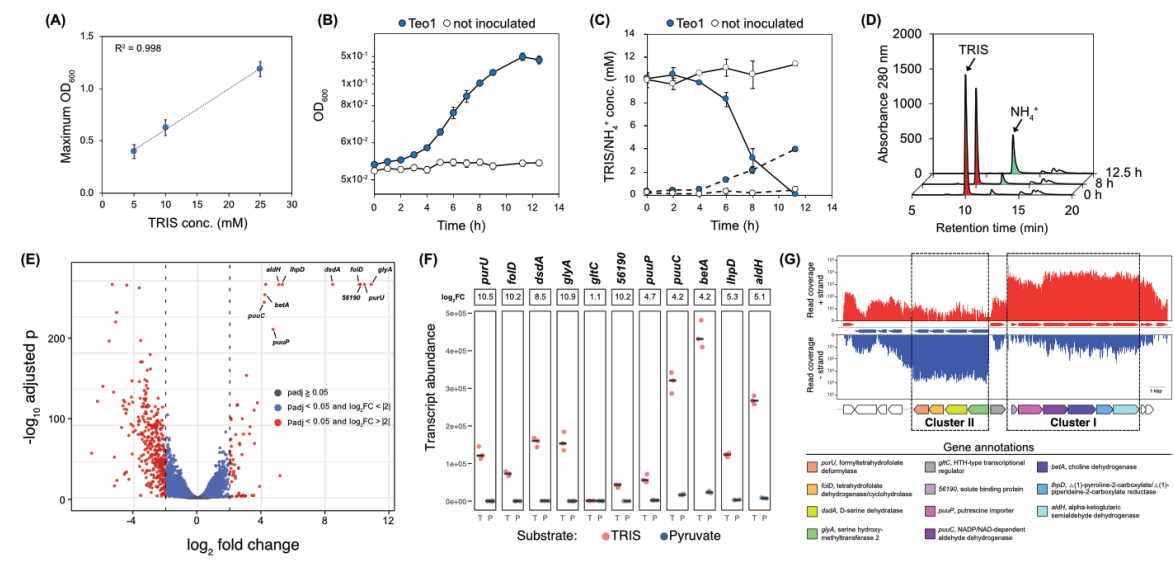

Fig. 1: Characteristics of TRIS metabolism in *Pseudomonas hunanensis* Teo1 and identification of potential TRIS degradation genes. (**A**) Maximal biomass production of strain Teo1 in relation to TRIS concentration. Error bars indicate standard deviation (n = 3). (**B**) Growth of strain Teo1 with 10 mM TRIS as only carbon and nitrogen source (n = 6). (**C**) Removal of TRIS (straight lines) and formation of ammonium (dashed lines) in Teo1 growth cultures. (**D**) Representative HPLC chromatograms of a strain Teo1 culture growing with 10 mM TRIS. TRIS is depleted from the culture while ammonium is released. (**E**) Volcano plot of transcriptome data showing significantly up-regulated genes (red) under TRIS-grown (positive fold changes) and pyruvate-grown conditions (negative fold changes) in Teo1. Genes predicted to be involved in TRIS degradation are labelled. (**F**) Transcript abundances and $\log_2$(fold changes) of the predicted TRIS degradation genes in Teo1 in TRIS- and pyruvate-grown cells (three biological replicates of each growth substrate, horizontal bar indicates median, corrected p values of all selected genes were < 0.05). (**G**) mRNA reads (red: positive strand, blue: negative strand) of a representative TRIS-grown culture mapped onto the DNA section containing the predicted TRIS degradation gene clusters in strain Teo1.

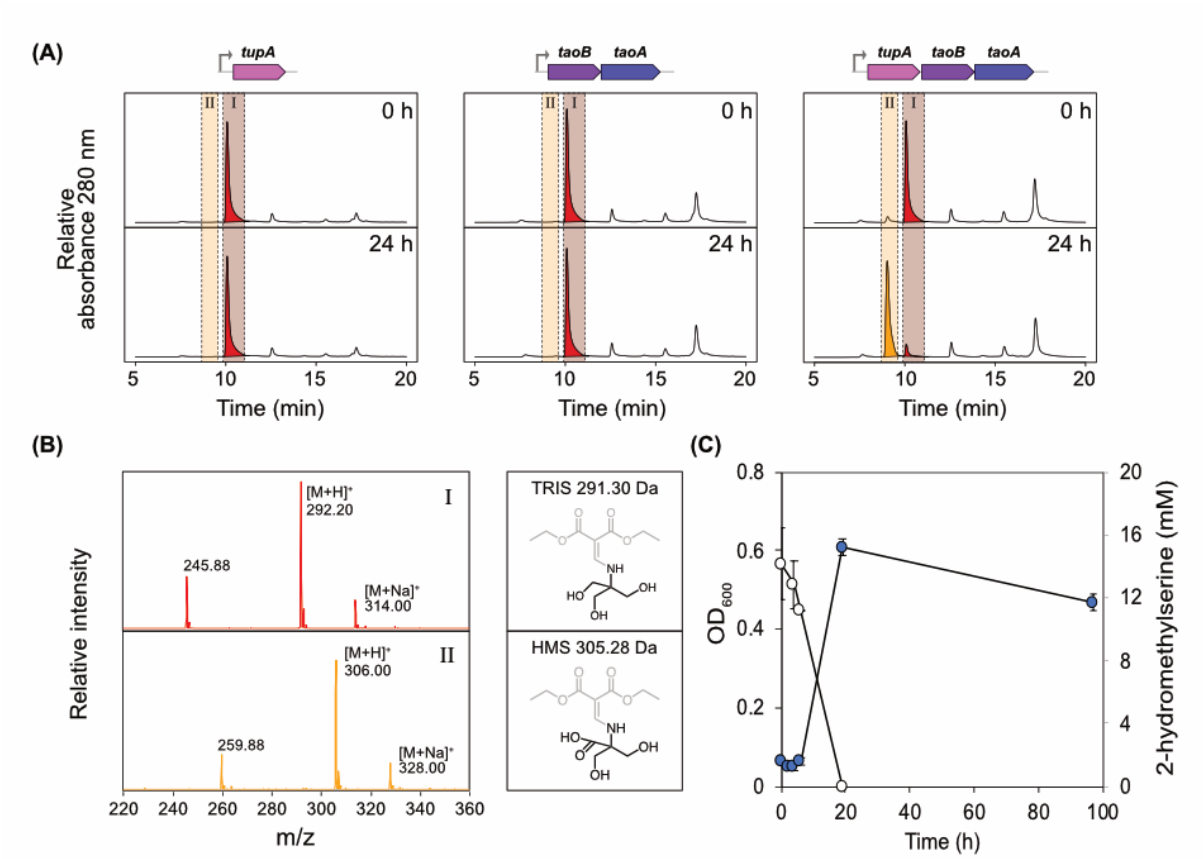

564
565 **Fig. 2:** TRIS transformation activity of *E. coli* strains carrying different combinations of the putrescine importer-
566 like protein-encoding gene (*puuP,* now *tupA*), the aldehyde dehydrogenase-encoding gene (*puuC,* now *taoB*), and
567 the choline dehydrogenase-like protein-encoding gene (*betA,* now *taoA*) on the expression plasmid pUCp18. (**A**)
568 Representative HPLC-UV/Vis chromatograms of TRIS-containing cell suspension supernatants of *E. coli* strains
569 that carried either the *tupA* gene, the *taoB* and *taoA* genes, or all three genes. TRIS (peak I, red) was transformed
570 into a new compound (peak II, orange) in the *E. coli* strain that carries all three genes only. The cloned genes were
571 under the activity of the *lac* promotor (grey arrow). (**B**) Mass spectra of TRIS (peak I) and the new product (peak
572 II). The new product was identified as 2-hydroxymethylserine based on the molecular mass of its diethyl
573 ethoxymethylenemalonate (DEEMM, grey molecule moiety) derivative of 305 Da, which is 14 Da heavier than
574 the molecular mass of 291 Da of the DEEMM derivative of TRIS. (**C**) Growth of strain Teo1 (blue circles) in
575 sterilized culture supernatants containing 2-hydroxymethylserine produced from TRIS and removal of 2-
576 hydroxymethylserine (white circles). Average and standard deviation of three independent biological replicates
577 are shown.
578

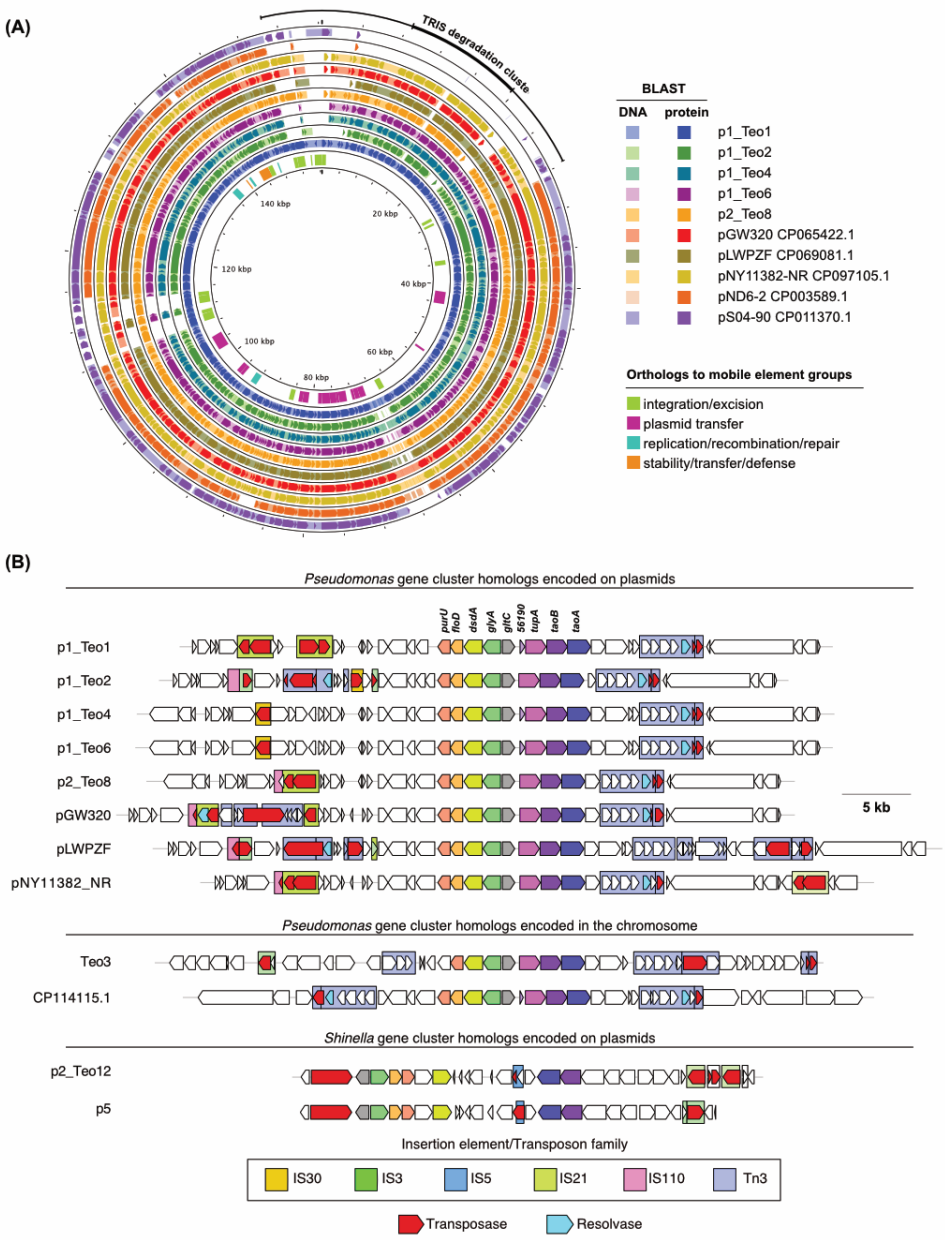

Fig: 3: TRIS degradation gene clusters in the genomes of the sequenced TRIS-degrading isolates from this study and of homologous gene clusters found in the NCBI nr nucleotide database. (**A**) Most TRIS degradation gene clusters are located on large circular plasmids with high sequence similarities to the *Pseudomonas* plasmids pND6-2 and pS04-90, which lack the TRIS degradation clusters. The outer black line indicates the location of the putative mobile genetic element including the TRIS degradation genes. Like pND6-2 and pS04-90, the TRIS degradation-encoding plasmids encode orthologs to mobile elements groups (inner circle) including a type IVB secretion system and a type IV pilus for plasmid transfer as well as a type II toxin-antitoxin system. (**B**) All TRIS degradation gene clusters, including plasmid- and chromosome-encoded clusters, are flanked upstream and downstream by transposon- or insertion element-like structures. The plasmid p2_Teo12 from *Shinella* sp. strain Teo12 and the homologous plasmid p5 in a *Rhizobium* strain have no similarity to the other TRIS degradation-encoding plasmids, but also carry two gene clusters which encode homologs to the other TRIS degradation proteins.

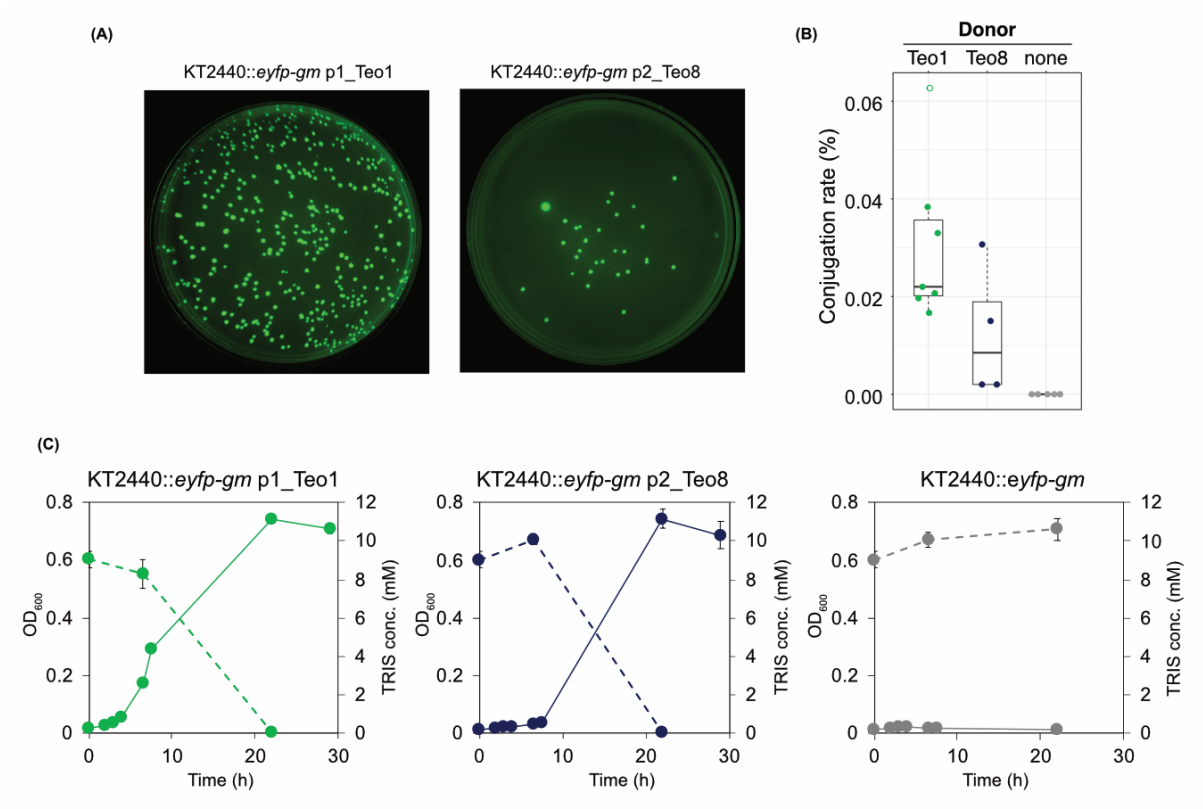

Fig. 4: Conjugative transfer of the TRIS degradation pathway-encoding plasmids p1_Teo1 and p2_Teo8. (**A**) Growth of YFP-fluorescing colonies on TRIS-containing agar plates after conjugation of *P. putida* KT2440::*eyfp-gm* with Teo1 (left panel) and Teo8 (right panel) as donor strains. (**B**) Conjugation rate of KT2440::*eyfp-gm* with p1_Teo1, p2_Teo8, and of a control without donor cells. Black lines indicate median rates of three independent conjugation experiments, boxes indicate the interquartile range, and dashed lines the maximum and minimum range. Transconjugants of up to seven replicates from three independent experiments were counted. Datapoints are coloured based on the donor strain. Outliers are not filled. (**C**) Degradation of TRIS (dashed lines) and growth (solid lines) of *P. putida* KT2440::*eyfp-gm* p1_Teo1 and p2_Teo8 transconjugants in liquid medium. The recipient strain *P. putida* KT2440::*eyfp-gm* without the conjugated plasmids was neither able to grow with, nor to degrade TRIS.

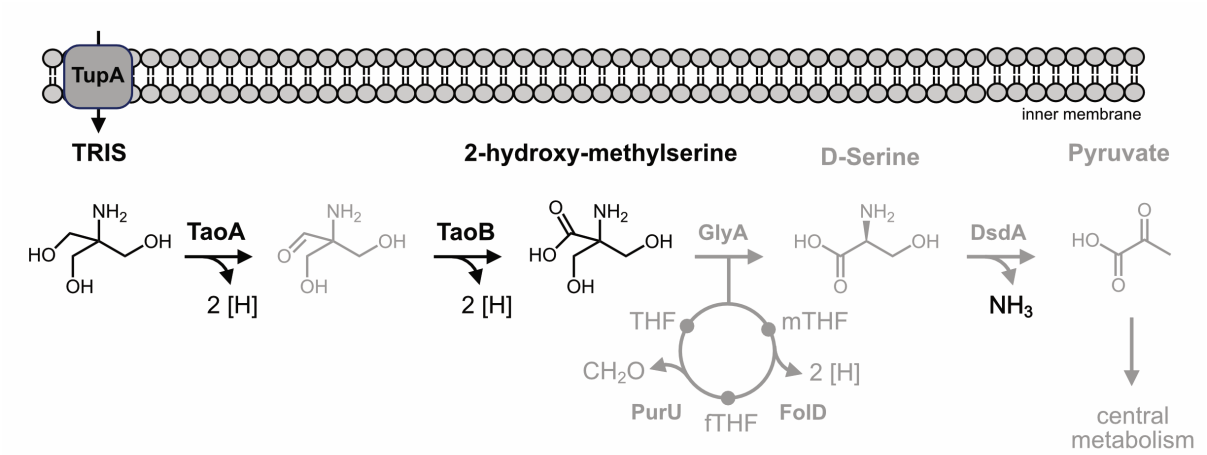

Fig. 5: Proposed TRIS degradation pathway. Confirmed reactions and intermediates are in black, proposed reactions and intermediates are in grey, THF = tetrahydrofolate, mTHF = methenyltetrahydrofolate, fTHF = formyltetrahydrofolate.